

Mechanical, Thermal, and Morphological Analysis of 3D-Printed Polylactic Acid–Polyester Urethane Blends with Varied Infill and Material Compositions

Suchetha N. Raju^{1,*}, S.H. Kameshwari Devi¹, K.P. Ajeya² and K. Prashantha²

¹Department of Polymer Science and Technology, Sri Jayachamarajendra College of Engineering JSS Science and Technology University, Mysure – 570006, India

²ACU-Centre for Research and Innovation, Adichunchanagiri School of Natural Sciences, Adichunchanagiri University, B.G. Nagara, Mandya District-571448, Karnataka, India

Abstract: Multimaterial 3D printing allows for the production of intricate parts with customized mechanical properties, enhancing the versatility of material extrusion additive manufacturing. Typically, 3D printing machines are fed with commercially available filament feedstock, which limits the 3D printing of multiple materials. Hence, this study introduces in-house prepared filaments for creating polymer blend structures with improved properties. In this study, polylactic acid and thermoplastic poly ester urethane (PEU) blends with different composition ratios were processed by varying the infill densities to evaluate their impacts on their thermal, mechanical and morphological properties. The effects of infill percentage on the mechanical, thermal and morphological behaviour were investigated. The results indicate that increasing the infill percentage tends to significantly increase the elastic modulus and tensile strength. The maximum strain increased as the infill percentage increased. Overall, the mechanical results indicated that, without sacrificing any tensile strength, the composite with 25% PEU exhibited better toughness than did the neat PLA and could be printed similarly to that of PLA. Furthermore, scanning electron images revealed that the blends had a homogeneous structure with a fibrillar morphology. These results indicate that 3D printing is an effective technique for creating next generation 4D materials.

Keywords: Additive manufacturing, 3D printing, Poly lactic acid, Thermoplastic polyurethane.

1. INTRODUCTION

Additive manufacturing (AM), popularly known as 3D printing, has transformed material processing in a greater manner. This fabrication method can produce intricate, customized, and lightweight structures with greater efficiency and design versatility. Among several additive manufacturing techniques, extrusion technologies such as fused deposition modeling (FDM) have gained prominence because of their unique capabilities, such as cost-effectiveness, extensive availability, and compatibility with various thermoplastic polymers[1-2]. The mechanical, thermal, and morphological properties of components generated by FDM are significantly influenced by the chosen material and manufacturing conditions. This has prompted flexibility tailoring material compositions and optimizing processing conditions to improve the performance of 3D-printed components [3-4]. In this context, two promising polymers—poly(ester urethane) (PEU) and polylactic acid (PLA)—have garnered attention due to their respective strengths and

complementary characteristics. PEU is a thermoplastic polymer synthesized by combining a diisocyanate, a chain extender, and a macrodiol (polyol), forming linear, segmented copolymers with alternating soft and hard domains [5]. The flexible soft segments, derived from polyols, contribute to elasticity, while the rigid hard segments impart mechanical strength and stiffness. This unique microphase-separated structure gives PEUs excellent mechanical tunability and thermal responsiveness, making them suitable for flexible biomedical devices such as artificial blood vessels, catheters, and cartilage replacements [6–8].

Conversely, PLA is a semicrystalline polymer derived from renewable resources such as corn, sugarcane, and beets. Composed of lactic acid monomers joined by ester linkages, PLA is widely recognized for its biodegradability, biocompatibility, and favorable mechanical properties [9-11]. PLA, composed of lactic acid monomers linked by ester linkages, is esteemed for its biodegradability, mechanical strength, biological compatibility, and manufacturing simplicity. These features have established PLA as a material of choice in biomedical fields, including sutures, implants, and drug delivery systems. However, unlike PEU, PLA lacks inherent flexibility and has limited deformability, restricting its

*Address correspondence to this author at the Department of Polymer Science and Technology, Sri Jayachamarajendra College of Engineering JSS Science and Technology University, Mysure – 570006, India; E-mail: suchetha@sjce.ac.in

application in scenarios requiring resilience and dynamic mechanical performance [12-14].

The mechanical performance of 3D-printed components is determined by material selection and critical processing factors such as infill density, raster angle, layer thickness, and printing speed [15]. The infill percentage and raster angle are crucial in determining mechanical behavior because they influence the internal structure and stress distribution [16]. Increased infill percentages often increase the tensile strength and stiffness, although modifications to the raster angle can improve the anisotropic characteristics and strain performance [17]. Therefore, a comprehensive examination of these characteristics is essential for enhancing the mechanical properties of 3D-printed polymer blends. Kaiyao Qian *et al.* [18] revealed that the use of 20 wt% carbon fibers (CFs) in PLA-PEU blends markedly improved their mechanical characteristics. This modification resulted in a 70.7% increase in tensile strength, a 184% increase in the flexural modulus, and a 50.4% improvement in the impact strength. Compared with neat PLA, the impact strength of the CF-reinforced composites is up to 1.92 times greater, making the PLA-PEU-CF composites particularly suitable for applications requiring a balance of stiffness and toughness.

Buys *et al.* [19] investigated PLA/PEU blends with various ratios—100/0, 72/25, 50/50, 25/75, and 0/100—produced via an internal mixer operated at 200°C and 50 rpm for 15 minutes. The PLA/PEU (50/50 wt%) blend displayed a continuous morphology, which notably increased the impact strength. Similarly, Jašo *et al.* [20] examined the effects of blend ratios on the biodegradability, mechanical properties, and morphology of PLA/PEU blends fabricated through an extrusion process. They reported that blends with a low PLA content (10–30 wt%) presented a globular PLA structure dispersed within the PEU matrix. Blends containing 40–50 wt% PLA developed a co continuous morphology, whereas those with higher PLA concentrations (60–80 wt%) experienced phase inversion, resulting in PEU forming globular structures dispersed in the PLA phase. Studies on PLA/PEU blends with varying ratios revealed that a higher PEU content enhances shape recovery and reduces PLA crystallinity. Notably, a 30/70 PLA/PEU blend demonstrated optimal performance, including 80% elongation at break and a 40% shape recovery ratio, making it suitable for self-tightening surgical knots [21]. The addition of 5 wt.% copolymer (PTC) reduced the PEU particle size within the PLA matrix, significantly

improving the impact strength to 31.1% and 68.5% increase compared with blends without PTC and pure PLA, respectively. However, excess PTC (>5 wt.%) led to decreased mechanical properties due to cluster formation, which diminished the effective compatibility. DMA analysis further validated the enhanced interaction between PLA and PEU in the presence of the copolymer PTC [22].

However, despite growing interest in PLA-PEU blends, most existing studies focus primarily on bulk processing methods like internal mixing and extrusion, with limited emphasis on their implementation in fused deposition modeling (FDM) using customized filaments. Furthermore, the combined effects of critical FDM processing parameters, such as infill density and raster angle, on the mechanical, thermal, and morphological performance of these blends remain underexplored. This study addresses this gap by systematically investigating the role of PLA-to-PEU ratios and key FDM settings in shaping the performance characteristics of 3D-printed components fabricated using in-house-prepared filaments. By addressing the limitations of commercially available filaments, the effects of varying PLA-to-PEU ratios and critical FDM processing parameters, such as infill percentage and raster angle, on the thermal, mechanical, and morphological properties of the blends were investigated. Detailed analysis of the tensile strength, elastic modulus, and strain revealed synergistic enhancements driven by the material composition and processing conditions.

2. MATERIALS AND METHODOLOGY

2.1. Materials

The present investigation utilized the PLA pellets (2003D) procured from Naturtech India Pvt. Ltd., Chennai, India and polyester urethane (demopan DP 2795A SMP), a polyester-based thermoplastic polyurethane (PEU) was purchased from Bayer Material Science AG. The material was dehumidified in an 80°C oven for 8 hours to remove absorbed moisture. This phase is essential for maintaining uniform material characteristics and avoiding flaws or inadequate interfacial bonding in later stages of processing.

2.2. Preparation of PLA/PEU Filaments

PLA-PEU mixtures with different content percentages were produced by processing the

granules in a twin-screw extruder at a screw speed of 60 rpm. The temperature throughout the zones, from the hopper to the die, was maintained between 190°C and 210°C to guarantee adequate mixing and melting of the ingredients. The extruded melt-blended substance was cooled in a water medium and subsequently pelletized. The pellets were dried overnight at 80°C to eliminate residual surface moisture and were then utilized for filament manufacturing. The desiccated pellets were subsequently utilized to manufacture filaments. The materials used were processed via a filament extrusion machine (Filabot EX2, Filabot, Barre, VT) at an extrusion temperature of 180°C to obtain filaments with a uniform diameter of 1.75 mm. The extruded filaments were gathered via a filament winder device (Filabot Spooler, Filabot, Barre, VT) prepared for subsequent application in additive manufacturing procedures.

2.3. 3D printing of Composite Filaments

The printing process was carried out via a Tvasta FDM printer (India) equipped with a nozzle diameter of 0.4 mm and operated at a nozzle temperature of 220°C. The printing speed was set at 30 mm/s for all test samples, with a layer thickness of 200 µm. To optimize the mechanical performance, the raster direction was aligned parallel to the stretching direction during printing.

2.4. Differential Scanning Calorimetry (DSC)

The thermal properties of the PLA/PEU blends, with sample weights ranging from 5 to 8 mg, were analyzed via differential scanning calorimetry (DSC1, Mettler, Switzerland). The samples were initially heated to 200°C at a rate of 10°C/min and held at this temperature for 5 minutes. Next, they were cooled to 25°C at the same rate and then reheated from 5°C to 200°C under identical conditions. The secondary melting curves were used to determine the characteristic temperatures and enthalpy values of the samples. Key parameters, including the glass transition temperature (T_g), cold crystallization temperature (T_{cc}), and melting temperature (T_m), were recorded. The crystallinity (X_c) of the PLA phase was calculated via Equation (1).

$$X_c = \frac{\Delta H_m + \Delta H_{cc}}{(1 - \omega_p) \Delta H_m^o} \quad (1)$$

Here, ΔH_m represents the enthalpy of melting, and ΔH_{cc} represents the enthalpy of cold crystallization.

ΔH_m is the theoretical enthalpy of melting for fully crystalline PLA (93.7 J/g), and ω_p denotes the mass fraction of PLA in the composites.

2.5. Dynamic Mechanical Analysis (DMA)

The dynamic mechanical properties of the PLA/PEU blends were evaluated via a MetraVib DMA system (France). Rectangular samples with dimensions of 35 × 5 × 2 mm³ were tested in single cantilever mode. The temperature was varied from 30°C to 100°C at a heating rate of 5°C/min, with a constant testing frequency of 10 Hz.

2.6. Mechanical Tests

Tensile tests were performed via a universal testing machine at a strain rate of 1 mm/min, following the ISO 527–2 standard. Dumbbell-shaped samples with dimensions of 75 × 10 × 2 mm³ were prepared through 3D printing for these tests. Impact tests were conducted in accordance with ISO 180, using rectangular samples with dimension of 80 × 10 × 2 mm³.

2.7. Scanning Electron Microscopy (SEM)

The cross-sectional morphologies of the 3D-printed PLA/PEU blend structures were examined via SEM (*Carl Zeiss Microscopy*) at an accelerating voltage of 15 kV. The cross-sectional surfaces were prepared by inducing brittle fracture in liquid nitrogen. Prior to imaging, the samples were sputter-coated with a thin layer of gold to enhance conductivity.

2.8. Wound Healing Assay

The wound healing assay, also known as the scratch assay, is commonly used to assess the migratory ability of cells following treatment. In this study, 3T3 cells—a fibroblast cell line derived from mouse Swiss embryo tissue—were cultured for the assay. A wound (scratch) was created using a sterile micropipette tip, after which the cells were treated with PLA/PEU (75/25) at concentrations ranging from 30 mg to 50 mg. Untreated cells served as the control. All samples were incubated in a CO₂ incubator, and images were captured at 0 hours and 24 hours post-treatment.

3. RESULTS AND DISCUSSION

3.1. Mechanical Properties

3.1.1. Tensile Strength and Elongation

The tensile moduli of the PLA/PEU (75/25) and PLA/PEU (50/50) blends are depicted in Figure 1a for 50, 75 and 100% infill densities. The figure clearly shows that the tensile modulus of PLA/PEU (75/25) is 40% greater than that of PLA/PEU (50/50) at 100% infill density. This substantial difference is attributed to the significant role of PLA, which has higher stiffness and strength than PEU does. The higher PLA content in the PLA/PEU (75/25) blend results in a stiffer matrix that can withstand more load under tension. On the other hand, in PLA/PEU (50/50), the increased PEU content softens the matrix, reducing its capacity to resist deformation and thereby reducing the tensile modulus.

An increase in the tensile modulus of 30% is observed for PLA/PEU (75/25) and 25% for PLA/PEU (50/50) when the infill density is increased from 50% to 100%. This is due to the reduction in the void fraction at higher infill densities. As the infill density increases, the material structure becomes more compact, improving stress transfer and thus minimizing the number of weak points in the matrix. However, the effect is stronger for PLA/PEU (75/25) because the material is naturally stiffer and benefits more from added continuity and material density. Thus, it is clear from the results that the tensile properties are mostly controlled by how much PLA is present in the blend and how well higher infill densities allow load to be transferred.

Figure 1b shows the percentage elongation of the PLA/PEU (75/25) and PLA/PEU (50/50) blends for 50, 75 and 100% infill densities, indicating the influence of the material composition and infill density on the elongation properties. Greater elongation was observed in the PLA/PEU (50/50) blend. This is because it has more polyether urethane (PEU), which is known for being flexible and able to stretch when stressed by increasing the PEU content, the blend becomes more ductile, allowing it to deform more before failure, resulting in greater elongation. On the other hand, the PLA/PEU (75/25) blend has more polylactic acid (PLA), which is a more fragile material that cannot stretch as much. This means that it cannot be stretched under the same conditions.

3.2. Impact Strength

The impact strength of the tested composite filaments is illustrated in Figure 2. In contrast to the tensile strength, the impact strength greater for PLA/PEU (50/50) than for PLA/PEU (75/25) at all infill densities, indicating the cooperation between stiffness and toughness in the composites. The impact strength of PLA/PEU (50/50) is 20% greater than that of PLA/PEU (75/25) at 100% infill density due to the elastomeric properties of PEU, increasing the toughness of the material, thus facilitating energy dissipation upon impact. The increased PEU concentration in PLA/PEU (50/50) results in a more ductile matrix, which can withstand more impact energy before breaking and experiencing plastic deformation. A higher PLA concentration stiffens PLA/PEU (75/25) and limits energy dissipation, reducing the impact strength.

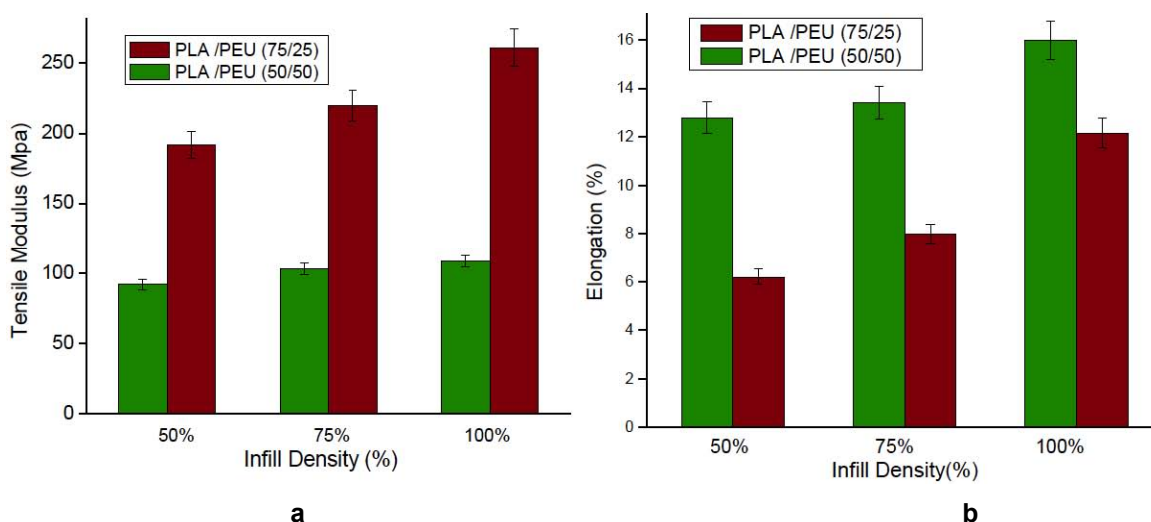


Figure 1: a) Tensile strength and b) elongation of the tested composite filaments.

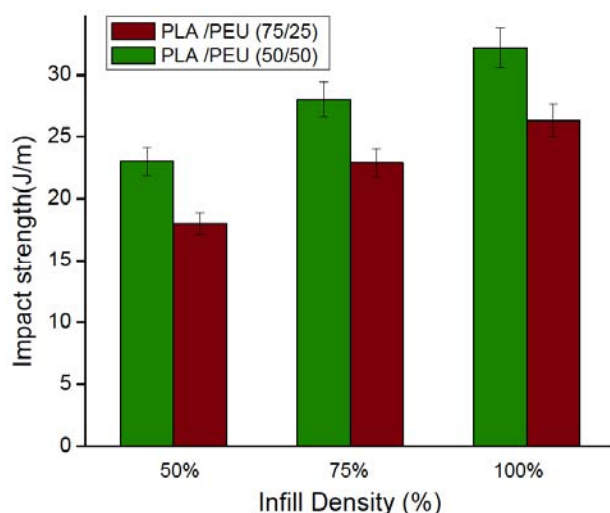


Figure 2: Impact strength of the tested composite filaments.

The impact strength markedly improved with infill density for both materials, with PLA/PEU (50/50) exhibiting a 50% enhancement and PLA/PEU (75/25) demonstrating a 40% enhancement as the infill density increased from 50% to 100%. Increased infill densities result in a more compact material structure, enhancing resistance to fracture initiation and propagation during impact. In PLA/PEU (50/50), the toughening effect of PEU is increased at elevated densities, allowing the material to dissipate more energy. Nonetheless, the enhancement is less evident in PLA/PEU (75/25) because of its more rigid matrix, which constrains plastic deformation.

The higher infill density of the impact strength for both tested blends resulted in 50% increases for PLA/PEU (50/50) and 40% for PLA/PEU (75/25). A higher infill density increases the compactness of the material increasing its resistance to impact fracture. This strengthening effect of PEU increases as the density of PLA/PEU (50/50) increases, resulting in more energy loss. This phenomenon is less apparent in PLA/PEU (75/25) because of its stiffness, which limits plastic deformation.

The differing responses of tensile and impact properties highlight the need to balance stiffness and toughness in polymer composites. Parameters such as the material composition infill density and interfacial bonding are vital. Tensile strength is primarily contributed by PLA, whereas toughness strength and impact resistance are contributed by PEU. The continuity in material and energy absorption is promoted by a higher infill density whereas the stiffness is improved by strong interfacial bonding.

3.3. Dynamic mechanical properties

Figure 3 presents the dynamic mechanical analysis (DMA) findings for a PLA/PEU (50/50) mixture, demonstrating the variation in the material's mechanical and thermal characteristics with temperature across various infill densities (IDs). The infill density values—100%, 75%, and 50%—are used to assess the influence of different amounts of structural reinforcement on the performance of the mixture. The study encompasses three principal parameters, namely, the storage modulus (E'), loss modulus (E''), and tan delta (δ), as illustrated in three distinct graphs.

Figure 3a) shows the storage modulus (E'), which quantifies the elastic properties of a material and its capacity to retain energy during deformation. This parameter is plotted versus temperature ($^{\circ}\text{C}$), with findings presented in MPa. At reduced temperatures, the storage modulus is elevated throughout all the infill densities, indicating that the material is rigid and resistant to deformation. As the temperature increases, the modulus markedly decreases, indicating a shift from rigid to more ductile conditions. The black curve, denoting 100% infill density, consistently demonstrates the largest storage modulus, whereas the red curve (50% infill density) displays the lowest values. This improved structural stiffness in the material is due to the increased infill density. The loss modulus (E''), which reflects the material's viscous behavior and capacity to dissipate energy as heat, is depicted in Figure 3b. The peak in the curve corresponds to the loss modulus to the glass transition temperature (t_g) of the PLA/PEU.

Compared with the green (75% ID) and red (50% ID) curves, the black curve (100% ID) shows the highest peak, indicating superior energy dissipation. This trend suggests that a higher infill density may lead to greater viscous responses due to increased internal friction and molecular motion within the material. Figure 3c displays tan delta (δ) which represents the ratio of the loss modulus to the storage modulus and provides information on the damping behavior of materials. The tan delta (δ) curves also reveal the glass transition temperature through prominent peaks. The black curve (100% ID) exhibited the most distinct and sharp peak indicating efficient dissipation and reduced damping over a narrow temperature range. In contrast, the broader peaks observed in the 75% and 50% infill density curves indicate increased damping and a more gradual transition from a stiff to a rubbery state.

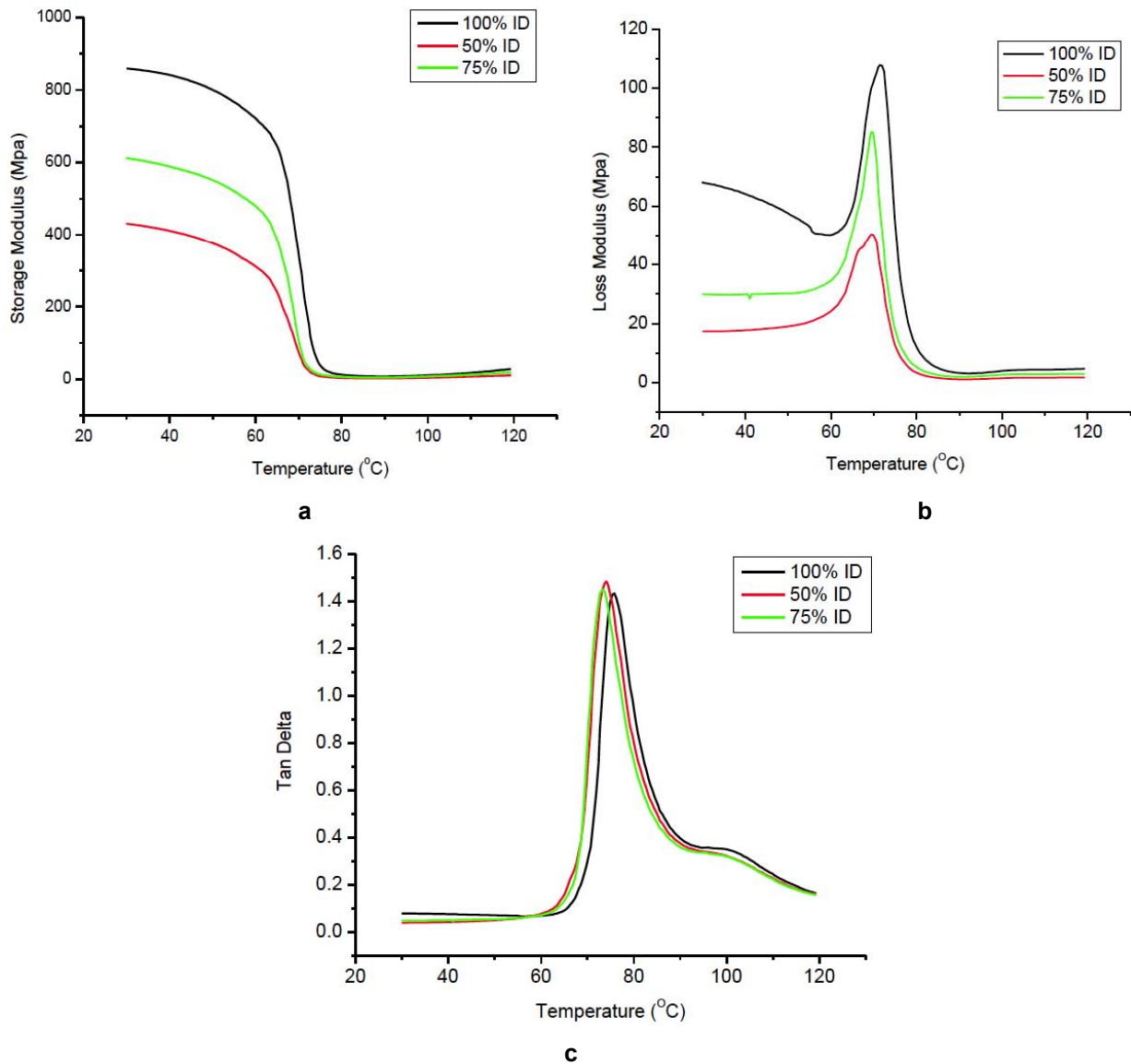


Figure 3: DMA curves for PLA/PEU (50/50).

a) Storage modulus (E') **b)** Loss modulus (E'') **c)** Tan delta (δ).

Figure 3(a-c) collectively highlights how infill density affects the mechanical and thermal behavior of PLA/PEU composites. Materials with higher infill density (100% ID) demonstrate enhanced structural stiffness, energy dissipation and damping efficiency, making them suitable for applications requiring higher mechanical strength and stability. Conversely, a low infill density (50% and 75%) results in materials with reduced stiffness but improved energy damping characteristics, which are advantageous for applications requiring flexibility and shock absorption.

The dynamic mechanical analysis (DMA) curves for a PLA/PEU (75/25) blend are shown in Figure 4. This figure shows how the material behaves thermally and mechanically at infill densities of 50, 75 and 100%,

demonstrating how the structural and thermal characteristics of the material are influenced by the infill density.

The storage modulus (E') of the tested blend is shown in Figure 4a. For all the tested infill densities, the storage modulus decreases with increasing temperature, indicating a transition from a rigid and glassy state to a flexible and rubbery state. The red line shows the highest storage modulus, indicating that the material is stiffer and more stable because of its denser structure. The 75% (black line) and 50% (green line) infill density curves, on the other hand, illustrate a decreasing storage modulus, indicating that the material is less stiff and stronger with decreasing infill density. This trend clearly demonstrates the importance

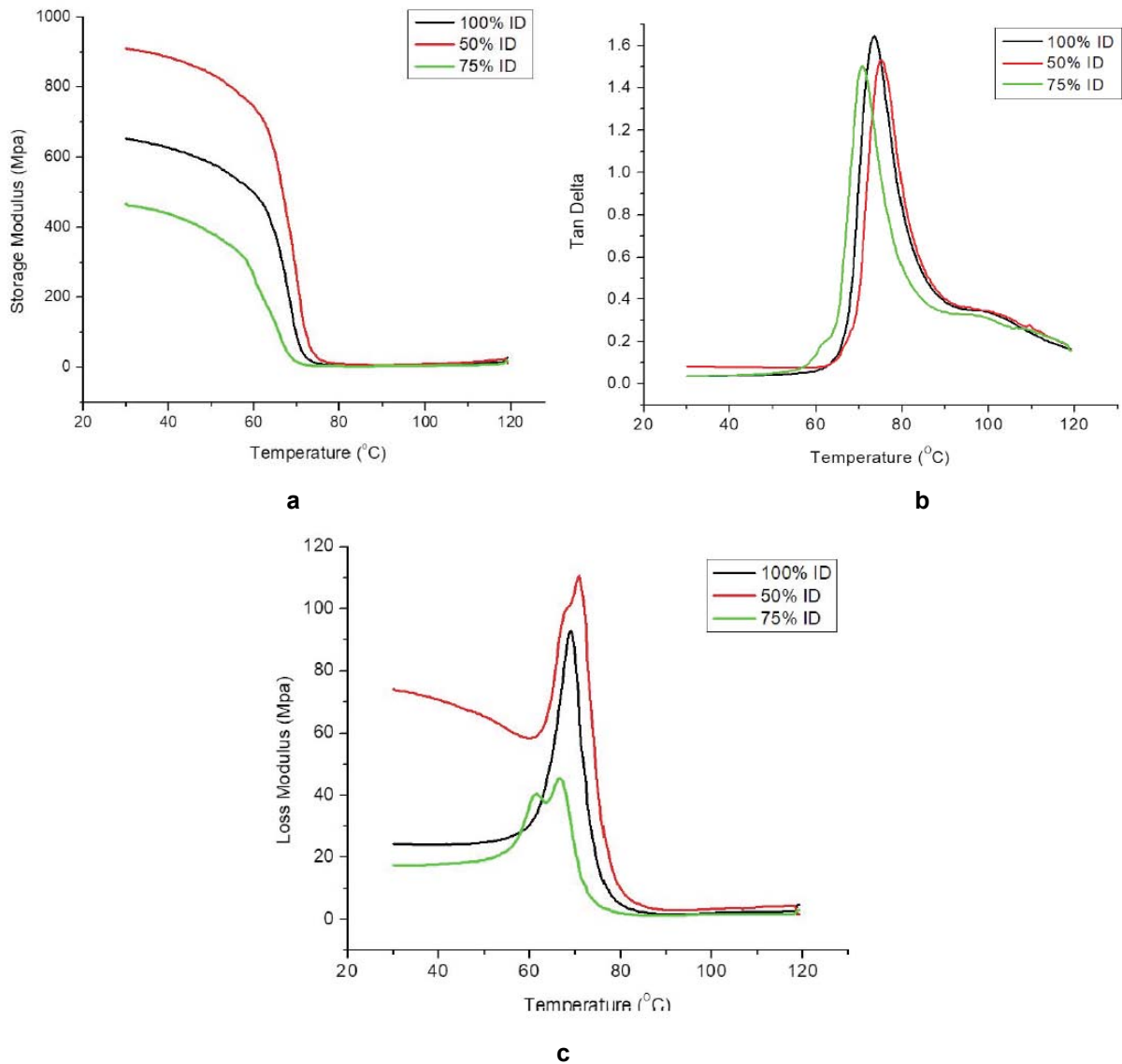


Figure 4: DMA curves for PLA/PEU (75/25).

a) Storage modulus (E') **b)** Tan delta (δ) **c)** Loss modulus (E'').

of higher infill densities for maintaining structural integrity.

The tan delta (δ), the ratio of the loss modulus to the storage modulus, is shown in Figure 4b. It indicates the material's glass transition temperature (T_g) and offers awareness of how it manages energy dissipation. The peaks in the tan delta curves, which represent the maximum molecular mobility of the material, are indicative of the T_g . Curve with 100% infill density

(red line) has the sharpest and most noticeable peak, indicating efficient absorption and dissipation of energy. The curves for the 50% (green line) and 75% (black line) infill densities, however, have wider,

less pronounced peaks. This indicates that they have a less transparent glass transition phase and are not effective at releasing energy.

The loss modulus (E''), which represents the viscosity and ability of a material to release energy as heat during deformation, is shown in Figure 4c. The loss modulus decreases as the infill density decreases, as observed with tan delta and the storage modulus. The 100% infill density (red line) with a maximum peak indicates increased energy dissipation and more noticeable viscous behavior. On the other hand, the curves for the 50% (green line) and 75% (black line) infill densities exhibit gradually decreasing peaks. The condition with the least amount of energy loss is 50% infill density. These results indicate that the ability of a

material to absorb energy and withstand mechanical strain during the glass transition phase is hampered by lower infill densities.

3.4. Differential Scanning Calorimeter Analysis

Figure 5 shows the thermal properties of the PLA/PEU blends examined via differential scanning calorimetry (DSC). The DSC results provide significant insights into the glass transition temperature (T_g), cold crystallization behavior, and melting properties (T_m) of various polymer blends. Understanding these transitions is vital for modifying their mechanical and thermal properties to meet the needs of certain applications. Figure 5a clearly shows that the glass transition temperature (T_g) is represented by the initial increase in the heat flow curve. A clear exothermic peak after the T_g indicates the occurrence of cold crystallization. In this phase, the application of heat causes the polymer's amorphous components to restructure into a more ordered crystalline structure. The endothermic peak at high temperatures denotes the melting point (T_m) of these crystalline regions, representing the thermal stability and crystalline structure of the material. The sharpness and intensity of the melting peak suggests that the PLA/PEU 75/25 mixture has high crystallinity, which changes the mechanical strength and thermal properties of the mixture.

Figure 5b shows similar temperature shifts, including glass transition, cold crystallization, and melting. However, these peak positions and sizes differ

from those of the 75/25 mixture, indicating the effect of the higher PEU concentration. Because of the higher PEU ratio, the T_g appears at a somewhat lower temperature, indicating greater chain mobility. The 50/50 mix appears to have healthier molecular mobility and a greater tendency for crystallization. This is because it has a wider temperature range and a stronger cold crystallization peak. Although the melting peak is not as strong as it is in the 75/25 blend, indicating a less stable or more dispersed crystalline structure. The PLA-to-PEU ratio has an extensive effect on the blends' thermal properties, as shown by the comparison of the two compositions. There is a clear melting point in the PLA/PEU (75/25) mixture, indicating that the crystallinity is better. Conversely, the PLA/PEU (50/50) mixture results in improved crystallization at lower temperatures, indicating that the molecular structure can rearrange more effectively and that the polymer chains gain greater flexibility when subjected to heat.

3.5. Morphology of the Blends

The SEM images of the PLA/PEU (75/25) composites in Figure 6(a-c) provide important insights into the structural and morphological characteristics resulting from the incorporation of a higher PEU content. Figures 6a and 6b illustrate the fractured surfaces of the composite. These images reveal a rough and irregular morphology, indicative of significant phase separation between the PLA and PEU phases. This observation suggests weak interfacial adhesion, likely due to the inherent immiscibility of the two

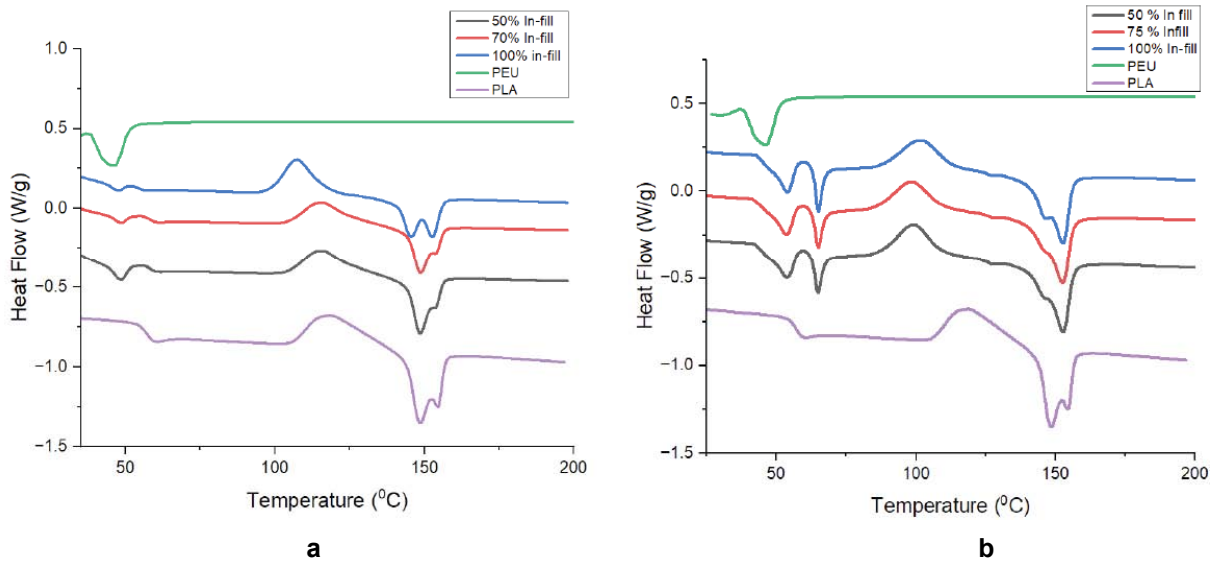


Figure 5: Crystalline and melting behavior of the PLA/PEU blended composite filaments. (DSC curves): a) PLA/PEU (75/25) b) PLA/PEU (50/50).

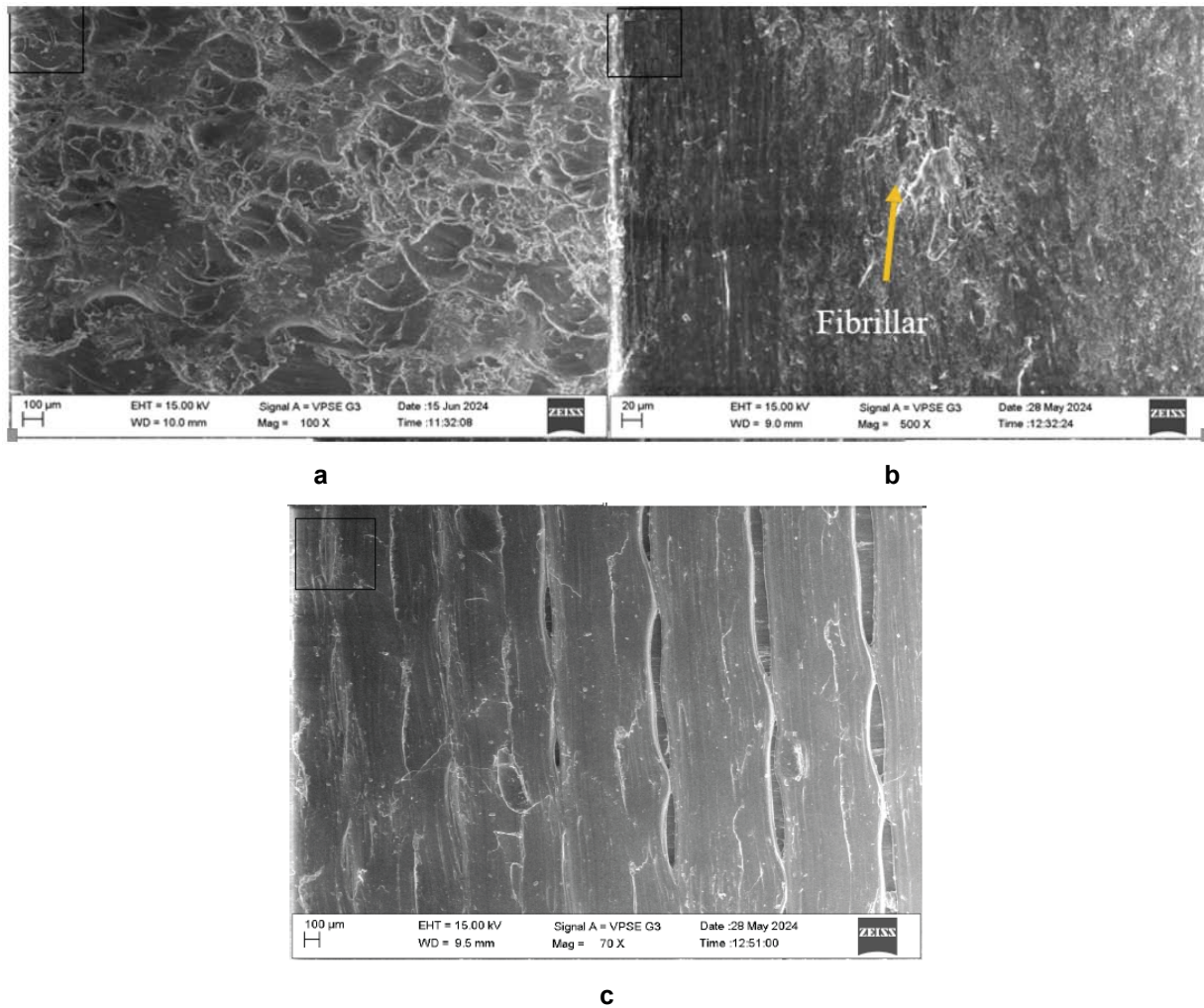


Figure 6: SEM images of PLA/PEU (75/25): **a)** 100%, **b)** 75%, and **c)** 50% infill density.

polymers at higher PEU concentrations. The distinct phase boundaries and the presence of micro voids may act as stress concentrators, reducing the overall mechanical strength and integrity of the composite. Distinct phase boundaries and the presence of microvoids averaging approximately 4–8 μm in diameter are apparent, which may act as stress concentrators and diminish the mechanical strength and integrity of the composite.

Figure 6c focuses on the longitudinal surface of the composite. The observed elongated cracks and heterogeneous regions highlight the challenges in achieving a uniform dispersion of PEU within the PLA matrix. These imperfections could result in nonuniform stress distribution under mechanical loading potentially compromised the structural performance of the composite. Additionally, the rough surface features observed across all the images are consistent with a brittle fracture mechanism, with possible localized ductile deformation due to the presence of PEU.

The higher PEU content in the composite may contribute to enhanced ductility and impact resistance, as PEU is known for its elastomeric properties. However, the observed microstructural heterogeneity underscores the need for improved processing strategies. For example, incorporating compatibilizers or employing advanced mixing techniques such as twin-screw extrusion or reactive blending could enhance the dispersion and interfacial bonding between the two phases.

The SEM images (Figure 7) of the PLA/PEU (50/50) composites provide valuable insights into their microstructural characteristics and material behavior. Figure 7a) reveals the fractured surface, revealing the surface morphology and distribution of PEU within the PLA matrix. Voids ranging from 3–10 μm in size, depending on the region are noticeable and may originate from inadequate interfacial adhesion or entrapped air during processing. Figure 7b) highlights the longitudinal section of the composite, offering a

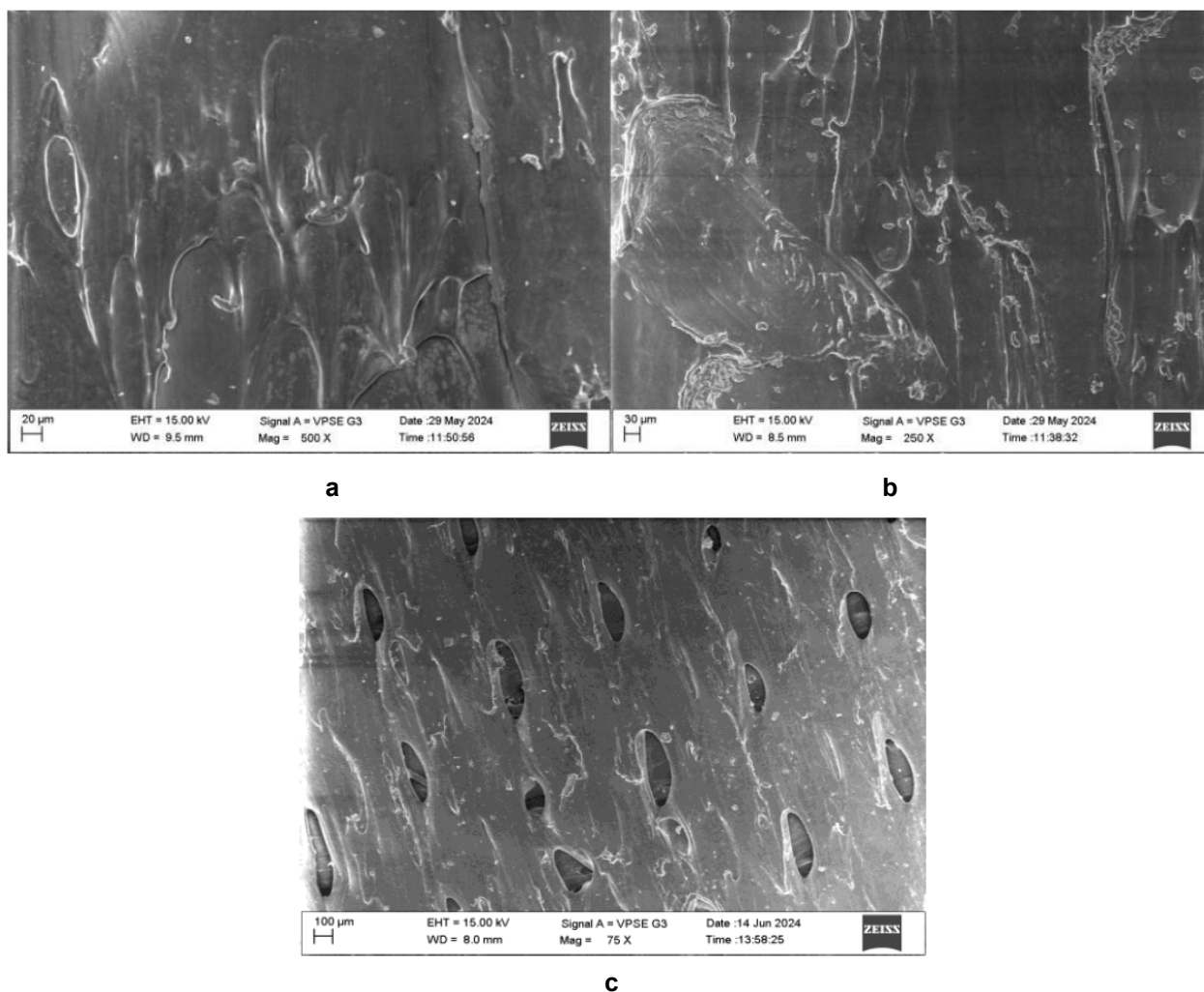


Figure 7: SEM images of PLA/PEU (50/50): **a)** 100%, **b)** 75%, and **c)** 50% infill density.

clear view of the fiber or polymer matrix orientation. Figure 7c) focuses on finer details, such as the presence of voids or imperfections within the matrix. These images indicate critical microstructural features, including porosity, phase separation, and cracks, which can provide clues about the material processing conditions and interfacial adhesion. The dispersion of PEU within the PLA matrix appears uneven, with possible signs of agglomeration that could influence the overall performance of the composite. Evidence of fracture mechanisms, such as the appearance of voids or smooth and rough surfaces, suggest a combination of brittle and ductile failure modes.

Quantitative microstructural assessments such as void size and crack morphology provide a clearer understanding of structure-property relationships. Future studies could benefit from correlating these SEM findings with mechanical performance data and comparing them against pure PLA or other PLA/PEU blend ratios.

The reduction in tensile strength or impact resistance may be due to the presence of voids and cracks. PEU incorporation may enhance toughness and elasticity, which is evident from the SEM images provided. Additionally, processing methods such as extrusion or injection molding likely play a significant role in shaping the composite microstructure. Variations in the cooling rate, shear force and mixing conditions may explain visible features such as voids or phase changes. These findings could be analyzed alongside SEM images of pure PLA or composites with different PLA/PEU ratios to better understand the influence of composition.

3.6. Scratch assay for PLA/PEU blends in 3T3 adipocyte cells

The scratch assay results were used to assess the cell proliferative activity of the blends, and it was observed that the PLA/PEU(75/25) blends led to an increase in fibroblast proliferation. Figures illustrate the

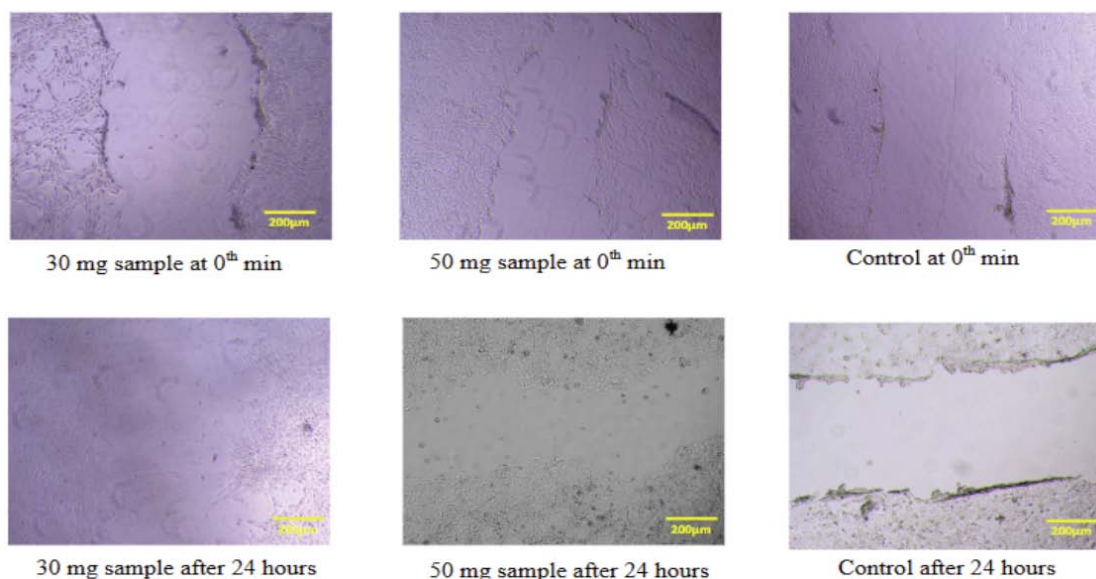


Figure 8: Scratch assay test for PLA/PEU blends in 3T3L adipocyte cells.

impact of the blends on 3T3L adipocytes. The images of the cells revealed that after treatment with the blends, the adipocytes remained viable, and no damage was caused to the cells, indicating their cytocompatibility.

4. CONCLUSION

This study's results offer substantial insights into the mechanical, thermal, and morphological characteristics of PLA/PEU composite filaments with different compositions and infill densities. The following conclusions may be drawn:

The percentage elongation was increased predominantly by 40% by increasing the ratio of PEU in the mixture of PLA/PEU (50/50). The tensile characteristics are predominantly influenced by the ratio of PLA in the mixture with the PLA/PEU (75/25) composite which has a 40% greater tensile modulus than does PLA/PEU (50/50) at 100% infill density. An increased PLA concentration yields a more rigid matrix that can endure higher loads. The impact strength increases with increasing PEU content. The impact strength of the PLA/PEU (50/50) composite was 20% greater than that of PLA/PEU (75/25) at 100% infill density because the elastomeric properties of PEU enhance energy dissipation during impact.

DMA revealed that increased infill density improved the structural rigidity, energy dissipation and damping capabilities of the composites. The 100% infill density resulted in an enhanced storage modulus, loss modulus and tan delta value which significantly

improved the mechanical stability and energy absorption. The glass transition temperature (T_g) and damping characteristics varies with the modification in composition and infill density. The PLA/PEU (50/0) has shown the enhanced flexibility and damping efficiency for increased elastomeric content.

The DSC study revealed the specific thermal transition which include cold crystallization and melting temperature (T_m) for the composites. The PLA/PEU (75/25) combination demonstrated enhanced crystalline and thermal stability which is more appropriate for requiring higher rigidity and thermal stability. Whereas PLA/PEU (50/50) shown the increased molecular mobility and cold crystallizations indicating increased flexibility and adaptability.

SEM revealed the difficulties in attaining uniform dispersion and robust interfacial bonding between PLA and PEU. The PLA/PEU (75/25) composites had notable phase separation, micro voids and characteristics of brittle fracture, whereas the PLA/PEU (95/5) composites revealed indications of agglomeration and void that affected the materials mechanical properties.

This finding highlights the necessity for enhanced processing strategies such as the use of sophisticated mixing process to augment the homogenizations and interfacial adhesion of PLA/PEU composites. The research has indicated that the mechanical, thermal and morphological characteristics of PLA/PEU composites are significantly influenced by the blend content and practical applications. The results offer

significant insight for enhancing the composition, manufacturing and structural design of PLA/PEU composited for various industrial and technical applications. More research on compatibilization procedure and innovative production process to improve the overall performance of these composites is recommended.

PLA/PEU composites show strong potential for targeted applications, depending on blend composition. The PLA/PEU (50/50) blend offers enhanced flexibility, damping, and porosity, making it suitable for biomedical scaffolds. Its elastomeric nature also makes it ideal for flexible wearable devices. In contrast, the PLA-rich PLA/PEU (75/25) blend provides higher rigidity and thermal stability, better suited for structural applications requiring mechanical strength. Future work should focus on developing hybrid composites with nanoclays, carbon nanotubes, or bioceramics could expand functionality. Scaling up via industrial methods such as twin-screw extrusion is key for commercial use. Further research into biodegradable compatibilizers, additive manufacturing optimization, and post-processing can help tailor properties for specific end uses.

REFERENCES

- [1] Ngo TD, Kashani A, Imbalzano G, Nguyen KT, Hui D. Additive manufacturing (3D printing): A review of materials, methods, applications and challenges. *Compos Part B Eng* 2018; 143: 172-96. (Google Scholar) <https://doi.org/10.1016/j.compositesb.2018.02.012>
- [2] Hajare DM, Gajbhiye TS. Additive manufacturing (3D printing): Recent progress on advancement of materials and challenges. *Mater Today Proc* 2022; 58: 736-43. (Google Scholar) <https://doi.org/10.1016/j.matpr.2022.02.391>
- [3] Ashrith HS, Jeevan TP, Divya HGV. 3D Printing of Crystalline Polymers. In: *Polymer Crystallization: Methods, Characterization and Applications* 2023. p. 233-54. (Google Scholar) <https://doi.org/10.1002/9783527839247.ch9>
- [4] Xiu H, Zhou Y, Dai J, Huang C, Bai H, Zhang Q, et al. *RSC Adv* 2014; 4: 37193. (Google Scholar) <https://doi.org/10.1039/C4RA06836J>
- [5] Puttaswamy JT, Puttegowda M, TG YG, Vedavathi DH. Evolution and recent advancements of composite materials in rapid prototyping. In *Applications of Composite Materials in Engineering* 2025. p. 169-193. (Google Scholar) <https://doi.org/10.1016/B978-0-443-13989-5.00007-3>
- [6] Jaso V, Cvetinovic M, Rakić S, Petrović ZS. *J Appl Polym Sci* 2015; 131. DOI: 10.1002/app.41104. (Google Scholar) <https://doi.org/10.1002/app.41104>
- [7] Azarmgin S, Torabinejad B, Kalantarzadeh R, Garcia H, Velazquez CA, Lopez G, et al. *Polyurethanes and their biomedical applications*. *ACS Biomater Sci Eng* 2024; 10(11): 6828-59. (Google Scholar) <https://doi.org/10.1021/acsbiomaterials.4c01352>
- [8] Zhu G, Wu M, Ding Z, Zou T, Wang L. Biological properties of polyurethane: Issues and potential for application in vascular medicine. *Eur Polym J* 2023; 112536. (Google Scholar) <https://doi.org/10.1016/j.eurpolymj.2023.112536>
- [9] Chen Q, Mangadiao JD, Wallat J, Leon AD, Pokorski JK, Advincula RC. *ACS Appl Mater Interfaces* 2017; 9: 4015. (Google Scholar) <https://doi.org/10.1021/acscami.6b11793>
- [10] Ferreira RTL, Amatte IC, Dutra TA, Bürger D. *Compos Part B Eng* 2017; 124: 88. (Google Scholar) <https://doi.org/10.1016/j.compositesb.2017.05.013>
- [11] Santo J, Pradhik V, Kalakoti S, Saravanan P, Penumakala PK. Effect of composite processing technique on tribological properties of 3D printed PLA-graphene composites. *Tribol Int* 2024; 198: 109895. (Google Scholar) <https://doi.org/10.1016/j.triboint.2024.109895>
- [12] Hanon MM, Ghaly A, Zsidai L, Klebert S. Tribological characteristics of digital light processing (DLP) 3D printed graphene/resin composite: Influence of graphene presence and process settings. *Mater Des* 2022; 218: 110718. (Google Scholar) <https://doi.org/10.1016/j.matdes.2022.110718>
- [13] Banupriya R, Jeevan TP, Divya HV, Yashas Gowda TG, Manjunath GA. 3D printed graphene-reinforced composites: Opportunities and challenges. *Polym Compos* 2024. (Google Scholar) <https://doi.org/10.1002/pc.29068>
- [14] Rachaiah B, Puttaswamy JT, Nagaraju SB, Vedavathi DH. Investigation on the wear characteristics of 3D printed graphene-reinforced PLA composites. *Discov Mater* 2024; 4(1): 1-11. (Google Scholar) <https://doi.org/10.1007/s43939-024-00152-z>
- [15] Doshi M, Mahale A, Singh SK, Deshmukh S. Printing parameters and materials affecting mechanical properties of FDM-3D printed parts: Perspective and prospects. *Mater Today Proc* 2022; 50: 2269-75. (Google Scholar) <https://doi.org/10.1016/j.matpr.2021.10.003>
- [16] Lanzotti A, Grasso M, Staiano G, Martorelli M. The impact of process parameters on mechanical properties of parts fabricated in PLA with an open-source 3D printer. *Rapid Prototyp J* 2015; 21(5): 604-17. (Google Scholar) <https://doi.org/10.1108/RPJ-09-2014-0135>
- [17] Hmeidat NS, Brown B, Jia X, Vermaak N, Compton B. Effects of infill patterns on the strength and stiffness of 3D printed topologically optimized geometries. *Rapid Prototyp J* 2021; 27(8): 1467-79. (Google Scholar) <https://doi.org/10.1108/RPJ-11-2019-0290>
- [18] Qian K, Qian X, Chen Y, Zhou M. Poly(lactic acid)-thermoplastic poly(ether) urethane composites synergistically reinforced and toughened with short carbon fibers for three-dimensional printing. *J Appl Polym Sci* 2018; 135(29): 46483. (Google Scholar) <https://doi.org/10.1002/app.46483>
- [19] Buys YF, Ahmad MS, Anuar H, Mahmud MS, Nasir NAM. Mechanical properties, morphology, and hydrolytic degradation behavior of polylactic acid/thermoplastic polyurethane blends. *IJUM Eng J* 2020; 21(1): 193-201. (Google Scholar) <https://doi.org/10.31436/iiumej.v21i1.1051>
- [20] Jaso V, Glenn G, Klamczynski A, Petrović ZS. Biodegradability study of polylactic acid/thermoplastic polyurethane blends. *Polym Test* 2015; 47: 1-3. DOI: 10.1016/j.polymertesting.2015.07.011. (Google Scholar) <https://doi.org/10.1016/j.polymertesting.2015.07.011>
- [21] de Melo Morgado GF, de Moura NK, Martins EF, Escanio CA, Backes EH, Marini J, et al. Effect of blend ratio on thermal, mechanical, and shape memory properties of poly(lactic acid)/thermoplastic polyurethane blends. *J Polym Res* 2022; 29(12): 533. (Google Scholar) <https://doi.org/10.1007/s10965-022-03389-5>

- [22] Fang H, Zhang L, Chen A, Wu F. Improvement of mechanical property for PLA/PEU blend by adding PLA-PEU copolymers prepared via in situ ring-opening polymerization. *Polymers* 2022; 14(8): 1530. (Google Scholar)
<https://doi.org/10.3390/polym14081530>
- [23] Wu Y, An C, Guo Y. 3D printed graphene and graphene/polymer composites for multifunctional applications. *Materials* 2023. (Google Scholar)
<https://doi.org/10.3390/ma16165681>
- [24] Raths M, Bauer L, Kuettner A, Fischer S, Laumer T. Gradual error detection technique for nondestructive assessment of density and tensile strength in fused filament fabrication processes. *Int J Adv Manuf Technol* 2024; 131(7): 4149-63. (Google Scholar)
<https://doi.org/10.1007/s00170-024-13280-w>

Received on 15-04-2025

Accepted on 13-05-2025

Published on 14-06-2025

<https://doi.org/10.6000/1929-5995.2025.14.05>

© 2025 Raju *et al.*

This is an open-access article licensed under the terms of the Creative Commons Attribution License (<http://creativecommons.org/licenses/by/4.0/>), which permits unrestricted use, distribution, and reproduction in any medium, provided the work is properly cited.